JOURNAL OF MATERIALS SCIENCE 22 (1987) 1352–1358

Crack resistance curves of alumina at high temperatures

H. WIENINGER, K. KROMP*
Institut für Festkörperphysik, University of Vienna, A-1090 Vienna, Austria
R. F. PABST†
I.S.M.R.A. U.A.251 Université de Caen, France

Ceramic three-point bend specimens were pre-cracked in a displacement-controlled test in air at room temperature to form sharp cracks of different lengths. Critical stress intensity factors (K_{IC}) were then measured as a function of sharp crack length in a fast-fracture, load-controlled test at 900, 1000 and 1100° C. By means of these fast fracture tests, crack resistance curves (K_{IC} against crack length) were determined for two commercially pure aluminas of different grain size and for a debased alumina containing a glassy phase. The crack resistance curve for the pure, fine grained alumina proved to be flat at 900° C, as was found for room temperature. A steeply rising crack resistance was, however, observed for the pure coarse-grained alumina at 1100° C and for the debased alumina at 1000 and 1100° C. This rise in K_R curves is explained by friction effects of the cracked microstructure behind the crack front for the coarse grained alumina and by adhesive forces caused by the second phase behind the crack front for the debased alumina. These facts are proved by comparison to experiments on notched specimen and by annealing experiments. From the annealing experiments the size of the adhesive zone is estimated for the debased material.

1. Introduction

The brittleness of ceramics implies that the crack resistance R should be independent of crack length and that the fracture toughness is seen as a single parameter independent of specimen dimensions and experimental procedure. This is different from metallic materials, where it is well known that the crack resistance may depend strongly on crack length. This fact is attributed to an increasing size of a plastic zone at the tip of the crack under plane stress conditions, accompanied by macroscopic blunting at the onset of crack extension. A plastic zone of comparable size cannot be found in brittle ceramic microstructures and therefore the condition for the existence of a fracture toughness parameter (materials constant) as a function of yield stress, plastic zone size radius and specimen dimensions are not fulfilled.

It is therefore most surprising that, similar to metallic materials, a dependence of crack resistance (fracture toughness) on crack length has been found [1]. It is significant in that context that the phenomenon was observed only in the case where sharp natural cracks instead of narrow notches were introduced as crack starters. It could be proved [1, 2] that crack resistance curves evaluated with different notch depths behave completely flatly. In addition a paradoxon was detected [1] in so far as fracture toughness values measured using narrow notches were equal to or smaller than those found for sharp cracks. According to notch-stress concentration factor analysis the opposite has to be anticipated. Based on these first results a discussion has been developed about the reasons and the importance of raising crack resistance curves in ceramic materials.

2. First results and explanations

In an analogy to plasticity reactions the effect is explained by a "process zone" seen as a region of microcrack formation *ahead* of the crack tip [3]. The rising crack resistance is explained by a magnification of that "zone" with increasing crack length. Yet, a "process zone" necessary to explain the distinct increase of fracture toughness could not be detected. It was argued, therefore, [2, 4], that friction effects or adhesive forces *behind* the actual crack tip are more likely to be responsible for the effect. These arguments were supported by measurements with narrow notches which guarantee traction-free surfaces. Traction-free surfaces are also found with metallic materials at the onset of crack extension if macroscopic blunting occurs, thus simulating a narrow notch. Nevertheless, an increase of crack resistance is found due to plastic zone extension. As macroscopic blunting does not occur in ceramic materials, the cracked surfaces keep close together, which allows friction and adhesive forces to act even under load. One could then easily

* *Present address*: Max-Planck-Institut für Metallforschung, Seestraße 92, 7000 Stuttgart 1, Federal Republic of Germany.
†The death of Dr R. F. Pabst is sadly recorded. (On leave of absence from Max-Planck-Institut für Metallforschung, Seestraße 92, 7000 Stuttgart 1, Federal Republic of Germany).

0022–2461/87 $03.00 + .12

imagine that a "zone" of friction and adhesion *behind* the actual crack tip is enlarged as the crack extends. Phenomenologically this is very similar to the magnification of a plastic or "process zone" in front of a crack. The "zone" behind the crack reaches its final length if the crack opening, a certain distance behind the actual crack tip, becomes so large that the contact between the cracked surfaces is lost. It is easily realized that the length or rather the "effectiveness" of the "zone" behind the crack tip depends on

(a) microstructure and composition
(b) temperature
(c) test procedure (load controlled, displacement controlled, loading rate)
(d) crack velocity
(e) time (oxidation, annealing, transformation reactions).

In particular if at elevated temperatures viscous second phases act as a binder between the cracked surfaces, the temperature and the test procedure play a dominant role. Therefore it should be emphasized that to characterize the quality of the crack resistance behaviour, well defined experimental parameters thus are necessary. This is also a prior condition for comparing any results. Therefore, in this paper catastrophic failure is based on rapid loading conditions in a load controlled test, avoiding subcritical crack extension prior to critical failure. Other and forthcoming papers deal with subcritical, displacement controlled tests at elevated temperatures [5].

3. Materials

For the experiments different qualities of Al_2O_3 were used as listed in Table I. Two qualities are commercially pure, Al_2O_3-S denotes a debased quality with a certain glassy phase content. In a hexagonal structure internal stresses increase with grain size. Therefore microcracking and friction effects may be increased by increasing the grain size as it was shown in a previous paper referring to room temperature reactions [2]. This is not to be expected with small-grained commercially pure materials.

The glassy-phase material is thought to provoke adhesive effects behind the actual crack tip, which may depend strongly on temperature and loading rate [6, 7].

4. Experimental procedure

The experimental procedure includes the following steps:

(i) the precracking process
(ii) the crack length measurement
(iii) K_R curve evaluation
(iv) annealing experiments
(v) investigation of the fracture surface

The annealing experiments were conducted at various temperatures and annealing times to account for the annealing procedure of sharp cracks especially if glassy second-phase reactions take place. The area of annealing at the cracked surfaces was then measured and related to the quality of the K_R curve. Referring to the precracking process three-point bend specimens 7 mm × 2.5 mm × 40 mm in size (span width 30 mm) were notched to a normalized notch depth of 0.2 mm and then precracked in air at room temperature to the desired sharp crack lengths using a completely displacement-controlled test at a displacement rate of only 1 μm min^{-1}. The rate ws directly measured and controlled by a LVDT in contact to the lower specimen surface. The specimens were then unloaded. The crack lengths were measured using a side-light technique on both sides of the specimen. As shown in a previous paper [2] a comparison with (a) post-mortem investigations at the cracked surfaces and (b) direct visual observation of the crack extension gives nearly the same result in crack length. It is important to know, if crack branching occurs, the nature of the kinetics of subcritical crack extension during displacement. This too may be investigated thoroughly by direct visual observation. The measured sharp crack length together with the notch length was then used as the crack length a in the linear elastic equation of the form [8]

$$K_R = \frac{3PS}{2BW^2} a^{1/2} Y(a/W) \quad (1)$$

with

$$Y(a/W) = Y(\alpha) = \frac{1.99 - \alpha(1-\alpha)(2.15 - 3.93\alpha + 2.7\alpha^2)}{(1+2\alpha)(1-\alpha)^{1.5}} \quad (2)$$

where P is the critical load, S the span width, B the specimen thickness, W the specimen width and $Y(a/W)$ the correction function.

The measured apparent critical K_R data were then plotted against the normalized crack lengths a/W, giving the K_R curve. The linear elastic relation (1) implies that the cracked surfaces are traction free with the traction free crack length a but it does not account for friction effects, adhesive forces and annealing effects behind the measured crack tip. It also implies linear elastic behaviour in front of the actual (visually observed) crack tip, excluding relaxation processes.

The specimens where heated up to the test temperatures of 800, 900, 1000 and 1100° C within 10 min and cracked in a rapid load controlled test at a loading rate of 1000 N sec^{-1}. As it was found that healing

TABLE I Properties of materials

Material	Composition (wt %)	Grain size (μm)	Young's modulus, 20° (GPa)	Density (kg m^{-3})
Al_2O_3	97% Al_2O_3 + 3% SiO_2	9 to 11	360	3.82
Al_2O_3-fg	99.7% Al_2O_3 + 0.3% MgO	1	378	3.94
Al_2O_3-Al23	99.6% Al_2O_3 + 0.4% MgO	20 to 40	350	3.87

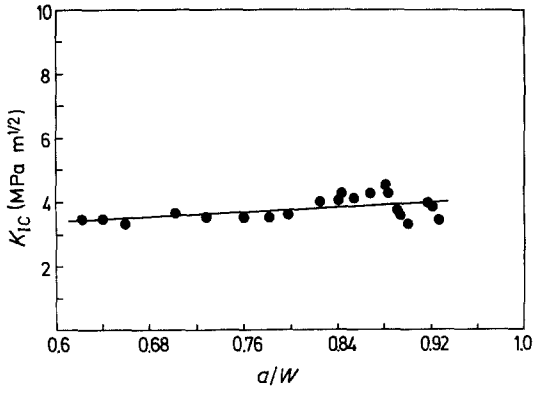

Figure 1 K_R curve for fine-grained pure alumina Al_2O_3-bio: Sharp pre-cracking and fast fracture in air at 900° C. The straight line has a slope of 1.9.

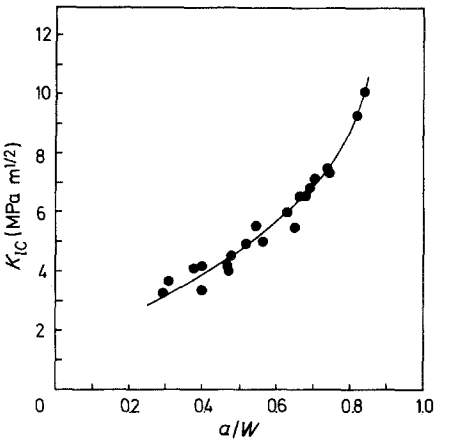

Figure 2 K_R curve for coarse-grained alumina Al_2O_3-Al23 in air at 1100° C: Sharp pre-cracking and fast fracture of pre-cracked specimens.

effects are likely to occur due to glassy phase reactions between the cracked surfaces, crack-annealing experiments were performed where the precracked specimens were tempered at 900, 1000 and 1100° C for 10 min, 4 h and 24 h and then fractured at room temperature. The fracture surfaces of the specimens were investigated by SEM.

5. Results and discussion

5.1. K_R curves as a function of temperature

The high temperature results are given in Figs 1 to 3. For a commercially pure and fine grained material (Al_2O_3-fg) a nearly flat K_R curve is measured at 900° C (Fig. 1). This is comparable to room temperature behaviour but with fracture toughness values at a lower level [2]. It is thus possible to define a single fracture toughness parameter at that temperature widely independent of crack length.

In contradiction to the behaviour above the coarse grained material Al_2O_3-A123 shows a distinct increase in fracture toughness which corresponds exactly to the room temperature behaviour [2]. Obviously even a test temperature of 1100° C does not change the friction reactions caused by the coarse grained microstructure (Fig. 2).

Compared to room temperature behaviour the K_R curve dependencies change tremendously if a fine-grained material with a second viscous phase is used (material Al_2O_3-S). The results are given in Figs 3a, b and c. First it is important to note that the fracture toughness values with notched specimens are completely independent of notch length, as anticipated. This is also the case for sharp cracks at the lower temperature of 900° C. However, increasing the temperature to 1000° C or even 1100° C, results in a steep increase of the K_R curve. The slope of the curve increases with increasing temperature. This steepness in slope is influenced by two effects:

1. the development of a certain region behind the crack front, where the second phase is activated during the time necessary for heating up (10 min)
2. by the level of the test temperature, which influences the dynamic activation of the second phase

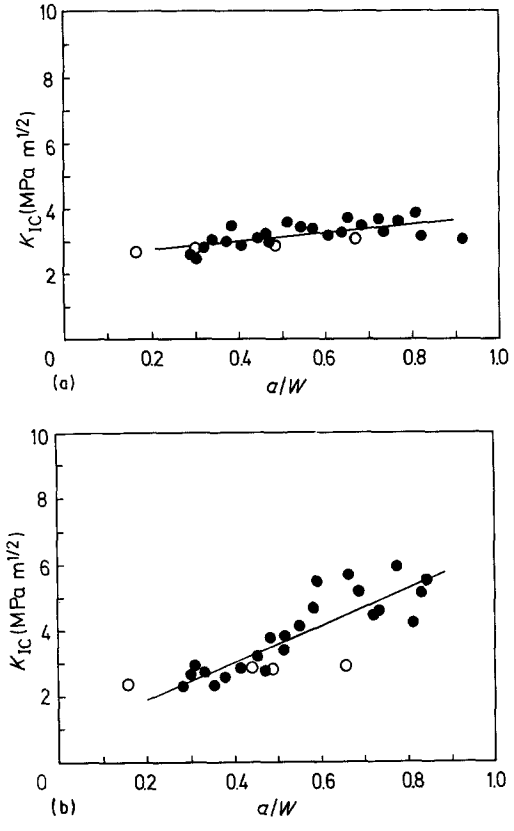

Figure 3 K_R curves for debased alumina Al_2O_3-S: Sharp pre-cracking and fast fracture of pre-cracked and notched specimens in air (●) K_R; (——) K_R slope; (○) K_{IC}, notched specimen. (a) 900° C; (——) K_R, slope 1.25 (b) 1000° C; (——) K_R, slope 5.7, (c) 1100° C; (——) K_R, slope 8.76.

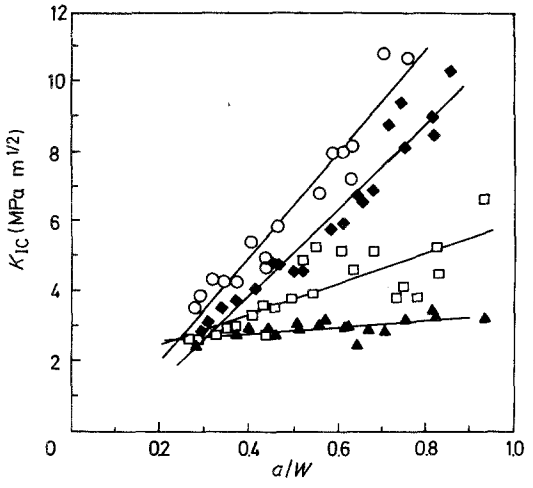

Figure 4 K_R curves for debased alumina Al_2O_3-S: Sharp pre-cracking, annealing at high temperature and fast fracture of pre-cracked specimens in air at room temperature (20° C). (▲) Annealing at 1000° C for 10 min, (□) annealing at 1100° C for 10 min, (◆) annealing at 1000° C for 4 h, (○) annealing at 1100° C for 4 h.

at the crack front during the test procedure at a constant high loading rate.

To investigate these dynamic effects during the test procedure and to give an estimation of the size of the active zone behind the crack front, annealing experiments were performed.

5.2. Annealing effects concerning material Al_2O_3-S

In the case of the material with the glassy phase a distinct annealing process was detected which depends on the holding time and the annealing temperature. Attention should be paid to the fact that the fracture toughness values were measured after cooling down to room temperature again to estimate the size of the active zone behind the crack front mentioned above.

For a short holding time of 10 min the K_R curve remains flat at an annealing temperature of 1000° C, whereas for 1100° C with this holding time a rising K_R curve is found (Fig. 4). Compared to the test results

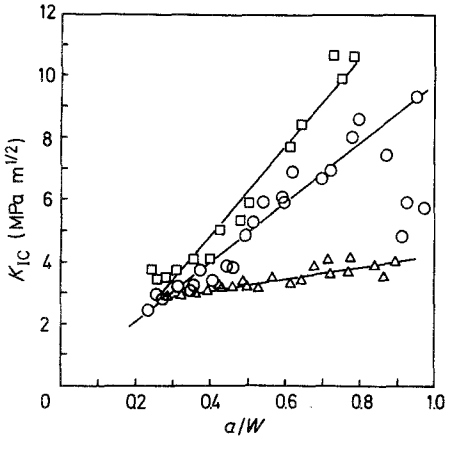

Figure 5 K_R curves for debased alumina Al_2O_3-S: Sharp pre-cracking, annealing at high temperature and fast fracture of pre-cracked specimens in air at room temperature (20° C). (△) Annealing at 900° C for 24 h, (○) annealing at 1000° C for 24 h, (□) annealing at 1100° C for 24 h.

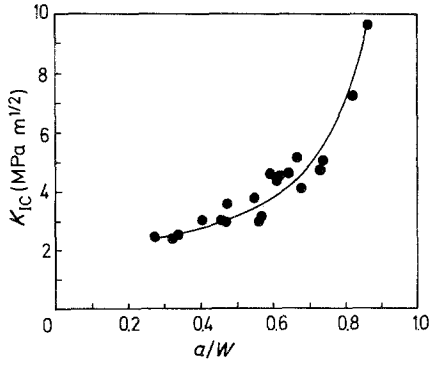

Figure 6 K_R curve for coarse-grained alumina Al_2O_3-Al23: Sharp pre-cracking, annealing at 1100° C for 24 h and fast fracture of pre-cracked specimens in air at room temperature (20° C).

from the last section (Figs 3b and c), the steepness is lowered, which indicates that with these room temperature tests only the reduction of the actual crack length by annealing is considered.

For a holding time of 4 h for both the annealing temperatures of 1000 and 1100° C K_R curves are found, rising to a high extent (Fig. 4). The slopes of the K_R curves at these temperatures were found to be similar to the longest performed holding times of 24 h (Fig. 5), whereas the effect of this holding time at 900° C is only small (compare Fig. 5 to 3a). The comparison with the dynamic tests at the elevated temperature exhibits a steeper increase for the case of annealing for 4 and 24 h and subsequent measurement at room temperature. From this it is obvious that the annealing of the sharp cracks and the development of the zone behind the crack front has a greater effect as the dynamic activation of the second phase during the test at elevated temperatures.

From these experiments and a post mortem investigation the size of the adhesive zone behind the crack front was estimated (see later on).

Concerning the course-grained material Al_2O_3-Al23 with no glassy phase, annealing experiments do not influence the K_R curve behaviour at all. Even an annealing temperature of 1100° C and 24 h holding time do not change the typical fracture toughness dependence measured at room- and elevated temperatures (compare Fig 2 to 6). It may be stated therefore that for annealing processes at temperatures and times used here, distinct reactions are only found if a second phase exists.

5.3. Crack length and crack velocity dependencies

As stated in the introduction the crack resistance behaviour additionally may depend on crack velocity and thus on the experimental procedure. This is the main reason to perform a well defined experimental procedure. In addition it was found [9] that the crack velocity in sharp cracked specimens may depend on crack length. Taking account for the results in Fig. 7 the crack velocity at a constant loading rate increases as the crack length decreases. This behaviour is obviously a function of the stored energy which is larger at shorter crack lengths thus resulting in larger initial

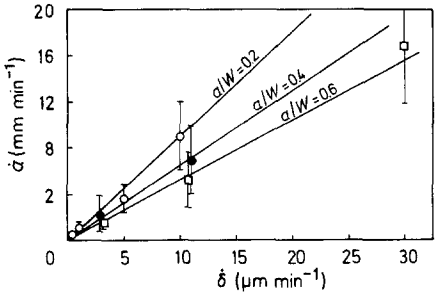

Figure 7 Dependence of crack velocity for debased alumina Al_2O_3-S at 1000° C on loading rate $\dot{\delta}$ for different crack lengths a/W.

velocities. This fact leads to lower fracture toughness values for the case of shorter crack lengths due to embrittlement reactions of the glassy phase at these high initial velocities. For this, even at a high constant loading rate in a load controlled test the rising K_R curve may at least partly be explained by embrittlement reactions due to different initial velocities.

Furthermore, if subcritical crack extension takes place before catastrophic failure occurs, the error in crack length measurement is comparatively larger with short than with long cracks, leading also to an apparent increase in fracture toughness with longer cracks. Those errors increase with decreasing viscosity at higher temperatures.

Apart from the reactions above which in any case are of a secondary nature, it is obvious that the increase of the measured fracture toughness as a function of crack length, temperature and annealing time must be attributed to adhesive and annealing effects *behind* the actual crack front. In particular if second phases exist, the cracked surfaces are not traction free even at the onset of fast fracture. The adhesive zone behind the actual crack tip increases with increasing crack length and temperature. Using Equation 1 which applies solely to traction-free surfaces, the fracture toughness is always overestimated. The overestimation increases with crack length and temperature. This is clearly revealed by the results evaluated with notched specimens, where stress-free surfaces are guaranteed (Figs 3a, b and c). At a certain load velocity in a load controlled test K_R curves with notched specimens behave flatly, independent of temperature. Therefore the formalism used is exactly appropriate to the narrow notch (notch width $\sim 70\,\mu$m) and not to a sharp natural crack, if adhesive or friction effects exist. Consequently, the difference between the measured notch-fracture toughness and that measured with sharp cracks may give a measure for the "length" or better the "effectiveness" of the adhesive zone z behind the actual crack tip.

If the Griffith formula

$$K_I = \sigma a^{1/2} Y \tag{3}$$

holds (which is not always clear if tractions behind the actual crack tip exist) a K_{Ieff} may be formulated such that

$$K_{Ieff} = \sigma a_{eff}^{1/2} Y \tag{4}$$

with

$$a_{eff} = a - z \tag{5}$$
$$z = z(\dot{a}, T, \text{composition})$$

where a is the actual measured crack length and Y the correction function. It is clear that in the case of viscous phases, z depends on the crack velocity $\dot{a}$, the temperature T and the composition.

Referring to the annealing effects in Al_2O_3, it may be anticipated that no macroscopic blunting exists, instead the sharp crack is filled with glassy phase, the extent of which depends on annealing temperature and time. The second phase gives a strong bond between the cracked surfaces after cooling down to room temperature. Depending on annealing temperature and annealing time the crack may be annealed to a great extent.

An attempt was made to evaluate the zone size z for the material with the second phase. For this the crack lengths were calculated for the experiments with the sharp natural cracks at 900, 1000 and 1100° C under the assumption that the K_R curves remain flat (compare Figs 3a, b and c). The difference between those crack lengths and the measured natural crack lengths gives a measure for this zone size.

The transformation of the Griffith equation results in a fourth order polynomial because of the correction function Y, which was solved for this purpose for relevant solutions in the range $0 < a/W < 1$ by interval-packing:

$$\frac{a}{W} Y^2(a/W) - \frac{4}{9} \frac{K_{IC}^2 B^2 W^3}{P^2 S^2} = 0 \tag{6}$$

where P is the load, S the span, B the depth and W the width.

These calculated zone sizes (mean values) are listed in Table II for $a/W = 0.4$, 0.6 and 0.8 at 1000 and 1100° C. At 900° C the rise in the K_R curve and thus the size of the zone is negligible.

TABLE II Evaluation for zone sizes z

Temperature (° C)	a/W	a_m measured (mm)	a_c calculated (mm)	$\Delta a = z$ (mm)	$\Delta a/a_m$ (%)
1000	0.4	2.8	2.48	0.32	11
1000	0.6	4.2	3.30	0.91	21
1000	0.8	5.6	4.81	0.79	14
1100	0.4	2.8	2.29	0.51	18
1100	0.6	4.2	2.68	1.52	36
1100	0.8	5.6	4.57	1.03	18

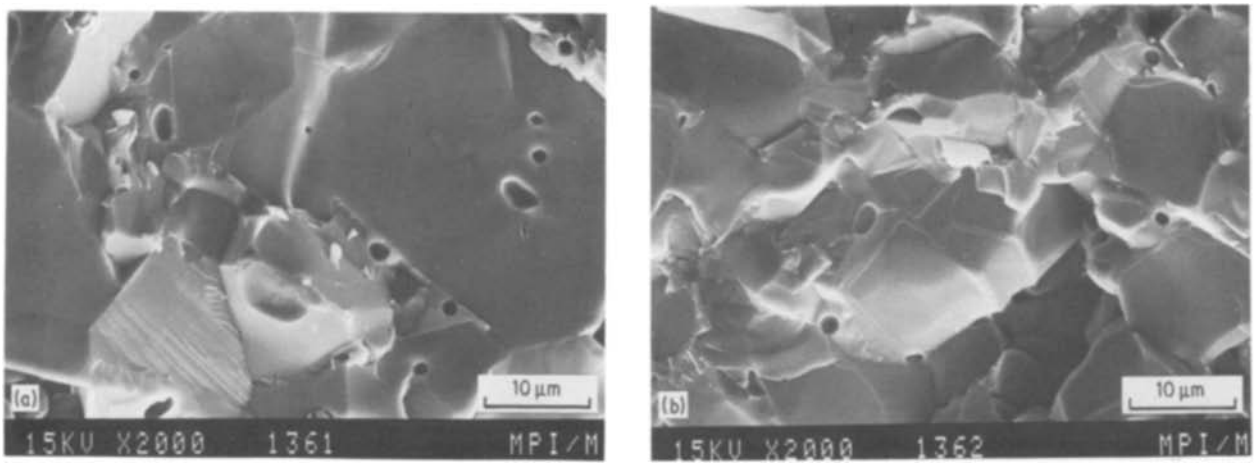

Figure 8 Fracture surface appearance of debased alumina Al_2O_3-S: Sharp pre-cracking, annealing at high temperature and fast fracture of pre-cracked specimens in air at room temperature (20° C), (a) Annealing at 1000° C for 10 min and (b) annealing at 1100° C for 10 min.

For $a/W = 0.4$ and 0.6, the z values show a rising tendency and realistic sizes compared to results from R-curve calculations with an energy concept [6]. For $a/W \geqslant 0.8$ the zone size is then obviously reduced again by the, for this case, high crack opening displacement. An investigation of the fracture surfaces in the range of the supposed zones was done by SEM on the specimens broken in the annealing experiments.

For a holding time of 10 min at 1000° C (10 min corresponds to the total holding time for all the high temperature experiments) the glassy phase coates the surface of the grains (Fig. 8a). At 1100° C the second phase concentrates in bands along the edges of the grains (Fig. 8b).

5.4. Annealing effects concerning material Al_2O_3-Al23

The data evaluated using the coarse grained material correspond well to room temperature measurements. Thus the friction effects behind the actual crack front are independent of temperature and annealing processes. Obviously this commercially pure material is insensitive to everything which does not influence the friction effects caused by the coarse-grained structure. Consequently experiments with notched specimens result in flat K_R curves, as was previously shown at room temperature [2].

5.5. High-temperature influence on material Al_2O_3-fg

The commercially pure fine grained material should be insensitive to friction effects (small grains, low internal stresses) and also to adhesive forces. Consequently as it is verified at least at 900° C, the K_R curve behaves flatly (Fig. 1).

6. Summary and conclusion

The distinct increase of crack resistance measured in a critical load-controlled test as a function of crack length at a distinct high loading rate is similar to that found with metallic materials under plane stress conditions. With metallic materials, however, a plastic zone of increasing size in front of the crack is made responsible for the increase in crack resistance. This is essentially different from reactions in ceramics found in this paper. It is stated that a plastic zone or any other "process zone" of microcracking in front of the crack tip does not exist. Instead, the cracked surfaces keep close together as no macroscopic blunting exists even at the onset of critical fracture. This allows friction and annealing and thus adhesive forces to act *behind* the actual crack tip. The surfaces therefore are not traction-free. A certain zone z of adhesion is formed behind the crack tip. Use of the well known Griffith equation based on traction free surfaces then leads to an apparent increase of fracture resistance. The problem remains in estimating the "length" or better the "effectiveness' of z which depends on microstructure, temperature and loading rate (crack velocity) and time especially if viscous second phases exist. From annealing experiments an attempt was made to evaluate the size of this zone z. In the simplest case the Griffith form may be used further with an a_{eff} instead of the actual measured crack length in an analogy to a plastic zone correction used for metallic materials. In any case the much more complex interactions of microstructure, temperature and loading rate in ceramics compared to metallic materials make it understandable that the test procedure itself plays a dominant role. This enlarges appreciably the experimental effects. Also the analytical verification becomes more complex as different ceramic materials behave much more individually at elevated temperatures. Simple analogies to metallic materials are misleading, assuming some sort of "process zone" in front of a crack. This analogy may be useful as a "working hypothesis", but does not account for the real effects which act behind the crack tips and not in front of them.

References

1. R. F. PABST, J. STEEB and N. CLAUSSEN "Fracture Mechanics of Ceramics", Vol. 4, edited by R. C. Bradt, D. P. H. Hasselman and F. F. Lange (Plenum Press, New York, 1978) p. 821.
2. H. WIENINGER, K. KROMP and R. F. PABST, *J. Mater. Sci.* **21** (1986) 411.
3. F. E. BURESCH, "Advances in Research on the Strength and Fracture of Materials", edited by D. M. R. Taplin, ICF4 Waterloo 1977 (Pergamon Press, New York, 1978) p. 939.

4. R. STEINBRECH, R. KNEHANS and W. SCHAARWÄCHTER, *J. Mater. Sci.* **18** (1983) 265.
5. T. HAUG and R. F. PABST, *J. Amer. Ceram. Soc.*, to be published.
6. A. BORNHAUSER, K. KROMP and R. F. PABST, *J. Mater. Sci.* **20** (1985) 2586.
7. R. F. PABST, K. KROMP, H. WIENINGER, A. BORNHAUSER and T. HAUG, *Fortschr. Ber. Deutsche Ker. Ges.* **1/3** (1985) 5.
8. J. E. SRAWLEY, *Int. J. Fract.* **12** (1976) 475.
9. T. HAUG, PhD thesis, University of Stuttgart (1985).

Received 30 May
and accepted 18 August 1986